Cancer Cell, Volume *16*

Supplemental Data

The B Cell Mutator AID Promotes

B Lymphoid Blast Crisis and Drug Resistance

in Chronic Myeloid Leukemia

Lars Klemm, Cihangir Duy, Ilaria Iacobucci, Stefan Kuchen, Gregor von Levetzow, Niklas Feldhahn, Nadine Henke, Zhiyu Li, Thomas K. Hoffmann, Yong-mi Kim, Wolf-Karsten Hofmann, Hassan Jumaa, John Groffen, Nora Heisterkamp, Giovanni Martinelli, Michael R. Lieber, Rafael Casellas, and Markus Müschen

Supplemental Experimental Procedures

In vivo model for BCR-ABL1-transformed ALL and bioluminescence imaging

CML cells were retrovirally transduced either with AID/GFP or GFP and subsequently labeled with lentiviral firefly luciferase. After transduction, 3 x 10^6 or 7 x 10^6 cells were injected i.v. into matched pairs of NOD/SCID recipient mice, which were sublethally irradiated with 250 or 350 cGy. In addition, 5 matched pairs of mice were intrafemorally injected with 3 x 10^6 AID/GFP- or GFP-transduced CML cells. After the injection of cells, the mice were imaged at different time points using the IVIS100 bioluminescence/optical imaging system (Xenogen, Alameda, CA). D-Luciferin (Promega) dissolved in PBS was injected i.p. at a dose of 2.5 mg/mouse, 15 minutes before measuring the light emission. General anesthesia was induced with 3% isoflurane and continued during the procedure with 2.5% isoflurane introduced via a nose cone. The Luminescent signal was analyzed as photons per second per cm^2 within the given region of interest with the Living Image 2.50 Software (Xenogen, Alameda, CA). Leukemia cell bioluminescence in mice is linearly correlated with the leukemia cell burden. Mice were monitored by bioimaging approximately on a weekly basis and also monitored for weight loss and other signs of disease. At the time of visible leukemia engraftment, mice where treated with 100 mg/kg Imatinib twice a day.

Ligation-mediated PCR for detection of DNA single-strand breaks

DNA break intermediates were amplified by ligation-mediated PCR (LM-PCR; Schlissel *et al*., 1992) with modifications for amplification of DNA single- in addition to double-strand breaks (Faili *et al*., 2002). DNA break intermediates in immunoglobulin V_H-DJ_H regions were amplified as a positive control. Genomic DNA from 2.5 x 10^6 cells containing a nick on the lower strand was denatured for 10 minutes at 95°C. Thereafter, and a gene-specific primer (Table S5) is hybridized and extended to the position of the nick, leaving a blunt end using Vent DNA polymerase (New England Biolabs, Beverly, MA). Next, a double-stranded linker is ligated to the newly created blunt end using T4 DNA ligase (Invitrogen) at 14°C overnight. The linker was constructed by annealing of the oligonucleotides 5'-TTTCTGCTCGAATTCAAGCTTCTAACGATGTACGGGGACATG-3'

and 3’ amino (C7)- GACGAGCTTAAGTTCGAAGATTGCTACATGCCCCT-5’ and protruding 3' overhangs were removed by 3'→5' exonuclease activity of the Klenow fragment of E. *coli* DNA polymerase I (Invitrogen). In two semi-nested rounds of amplification at an annealing temperature of 59°C, linker-ligated intermediates of DNA-single-strand breaks within various genes were amplified using gene specific primers together with two linker specific primers (Table S5).

Single Nucleotide Polymorphism (SNP) mapping assay and Comparative genomic hybridization

Genomic DNA was extracted from AID^{high} and AID^{low} Ph^{+} ALL samples (blast counts were higher than 80%) and subjected to 250K NspI SNP array analysis as described in the Supplementary Materials section., using the DNA Blood Mini Kit (Qiagen, Valencia, CA) and it was quantified using a Nanodrop Spectrophotometer. Quality was assessed using the Nanodrop and by agarose gel electrophoresis. The SNP mapping assay was performed according to the protocol of the manufacturer (Affymetrix, Santa Clara, CA). Briefly, 250 ng of DNA was digested with NspI (New England Biolabs, Boston, MA). Digested DNA was adaptor-ligated and PCR-amplified using Clontech Titanium *Taq* DNA polymerase (CELBIO) in three 100µl PCR reactions for each enzyme-digested sample. PCR products from each set of three reactions were pooled, concentrated and fragmented. Fragmented PCR products were then labeled, denatured and hybridized to the arrays. Arrays were then washed using Affymetrix fluidics stations, and scanned using the Gene Chip Scanner 3000. Cell files and corresponding SNP genotype call files were generated using Affymetrix GeneChip Genotyping Analysis Software (GTYPE) v 4.0. Affymetrix CEL files were analyzed for genomic copy number variations using Partek Genomic Suite software. Copy number aberrations were scored using the Hidden Markow Model (HMM). An alteration was defined as a region identified by the HMM algorithm and having a copy number state lower or higher than 2 based on at least 3 probesets. All aberrations identified were compared to those observed in a cohort of 48 Hapmap normal individuals in order to reduce the noise of raw copy number data. Alterations were then queried against established polymorphic genomic regions (http://projects.tcag.ca/variation/) to exclude copy number variations due to polymorphic alleles. Degrees of overlap among the remaining true aberrations were visualized subsequently using Partek Genomic Suite software. Copy number alterations were calculated separately for AID^{high} and AID^{low} Ph^{+} ALL samples.

Comparative genomic hybridization (CGH) of $AID^{-/-}$ and $AID^{+/+}$ BCR-ABL1 B lymphoid leukemia cells

Bone marrow cells from $AID^{-/-}$ and $AID^{+/+}$ mice were transduced with *BCR-ABL1*. After 9 weeks in cell culture, genomic DNA was isolated using Invitrogen PureLink Genomic DNA Kit (Invitrogen Carlsbad). Amplifications and deletions were determined using Mouse Genome CGH Microarray Kit 244A (Agilent Technologies, Inc., Santa Clara) using genomic DNA from normal splenic B cells as a reference. The hybridization and labeling was performed by MOgene (Saint Louis, MO). The data were analyzed using DNA Analytics 4.0 (Agilent Technologies, Santa Clara, CA). The normalization of the log values was calculated by

the centralization algorithm. The aberrations between the sample and the reference based on log2 ratios of fluorescent signals from probes in the interval were calculated using the AMD-2 aberration algorithm with a threshold of 6. The Fuzzy Zero algorithm was used as global error model. The standard aberration and feature level filters from DNA Analytics 4.0 were applied. Default feature level filter removes data for features that have a non-uniformity or saturated flag set for either channel. The aberration interval based report was confirmed by visual inspection of the raw data plots.

Figure S1: *Genomic organization of potential target genes of AID-mediated hypermutation in BCR-ABL1-driven B cell lineage leukemia*

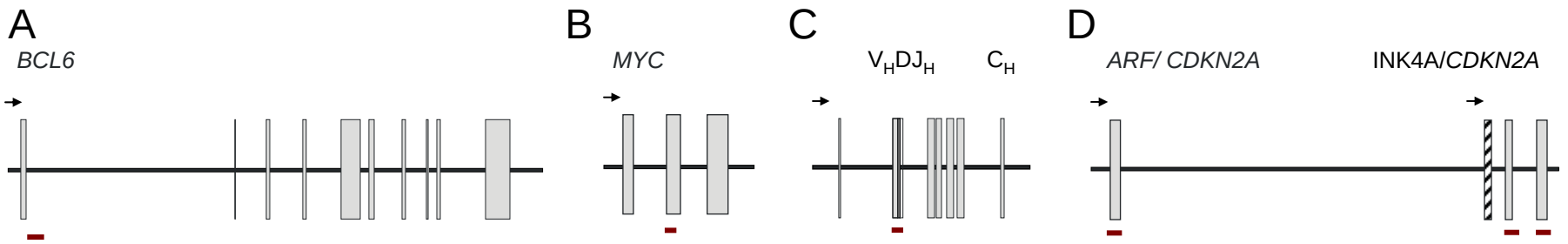

Sequence analysis was performed for the *BCL6* (A), *MYC* (B), *IGHM* (rearranged locus; C) and *CDKN2A* (ARF; D) genes. Gray boxes denote exons, arrows indicate the transcription start sites (TSS) and red bars indicate the region that was selected for sequence analysis.

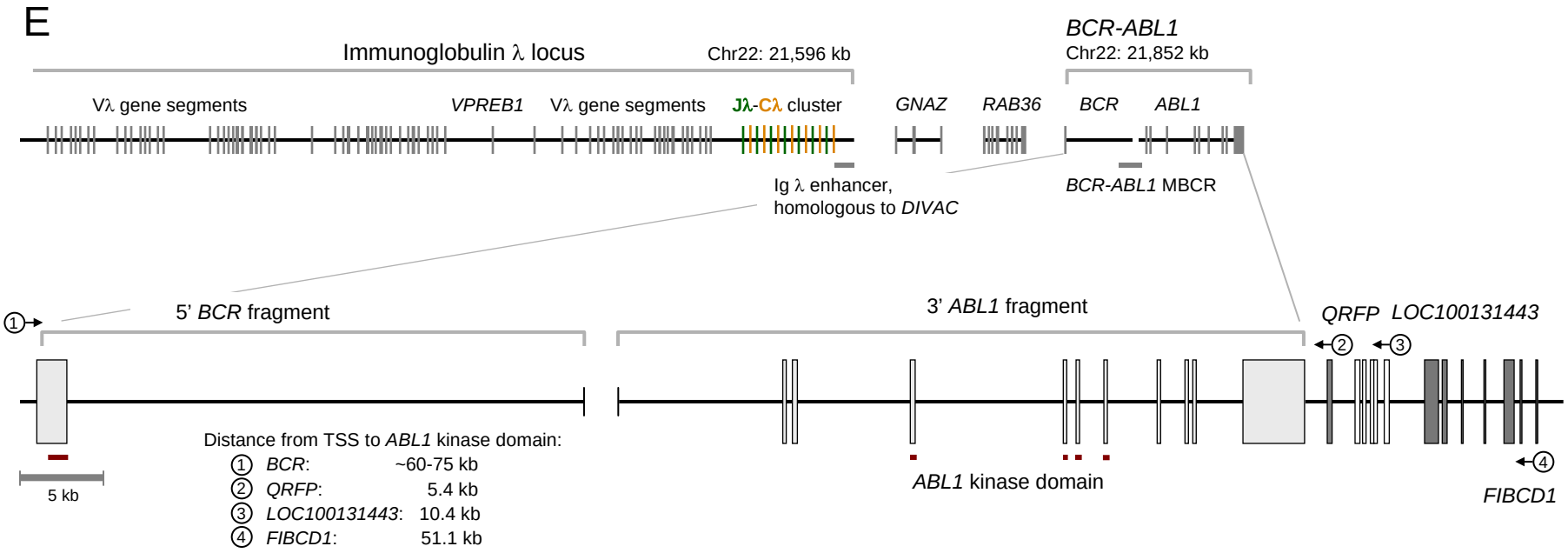

The upper panel depicts the regional context of the *BCR-ABL1* fusion gene at 22q11 relative to the immunoglubulin λ locus, *VPREB1* and homology regions to chicken *DIVAC* at the Ig λ enhancer (cis-acting element, Diversification Activator, induces AID-dependent hypermutation of Ig and Non-Ig genes; Blagodatski *et al.*, 2009). The MBCR (major breakpoint cluster region) is typically observed in CML and B lymphoid blast crisis of CML and encodes the p210 form of the BCR-ABL1 fusion protein (210 kD). The genomic organization of the *BCR-ABL1* fusion gene is depicted in the lower panel. Gray boxes denote exons, arrows indicate the transcription start sites (TSS) and red bars indicate the regions that were selected for sequence analysis. The distances from TSS of the *BCR*, *QRFP*, *LOC100131443* and *FIBCD1* genes relative to the *BCR-ABL1* kinase domain are indicated.

Figure S2: *Mutation analysis of the ARF/CDKN2A gene*

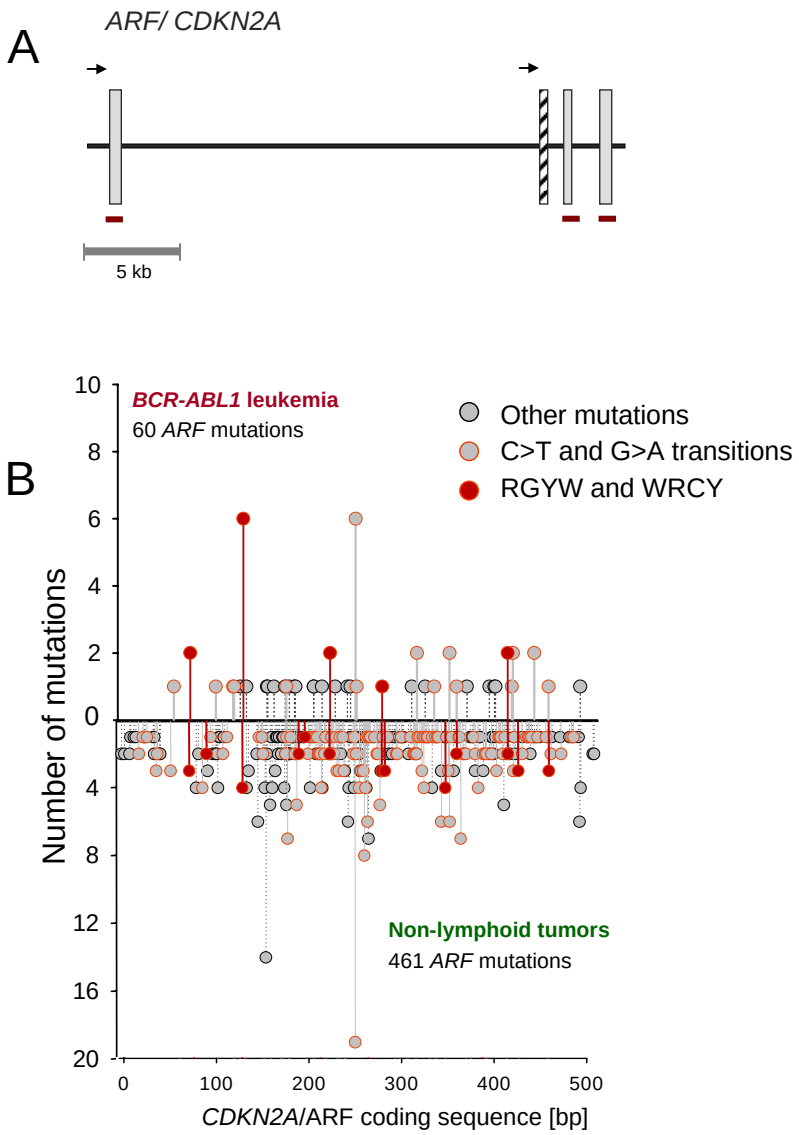

Legend:

The *CDKN2A* locus with two transcription start sites (arrows) is depicted in (A). Red bars denote the coding exons of ARF that were analyzed. Sequence analysis of the *ARF* coding sequence (471 bps) in *BCR-ABL1* driven B cell lineage leukemias (Ph^+ ALL and LBC, top) and non-lymphoid tumors (bottom) based on publicly available databases (see below). Mutations were classified as targeting RGYW or WRCY hotspot motifs (red circles), C>T and G>A transitions (orange circles), or others (gray circles).

Mutation data were obtained from:

1. https://biodesktop.uvm.edu/perl/p16
2. http://www.sanger.ac.uk/perl/genetics/CGP/cosmic?action=bygene&ln=CDKN2A

Figure S3: *Ectopic expression of AID in CML cells*

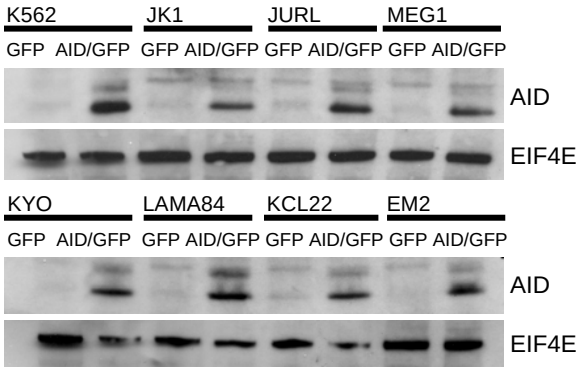

Legend. Eight AID- CML cell lines were transduced with a retroviral (MSCV) vector encoding AIDand GFP or GFP alone. Transduction efficiency was monitored by flow cytometry (GFP^+ cells, not shown) and ectopic expression of AID was verified by Western blot using EIF4E as a loading control.

Figure S4: *Ectopic expression of AID in CML cells induces Imatinib-resistance in vitro*

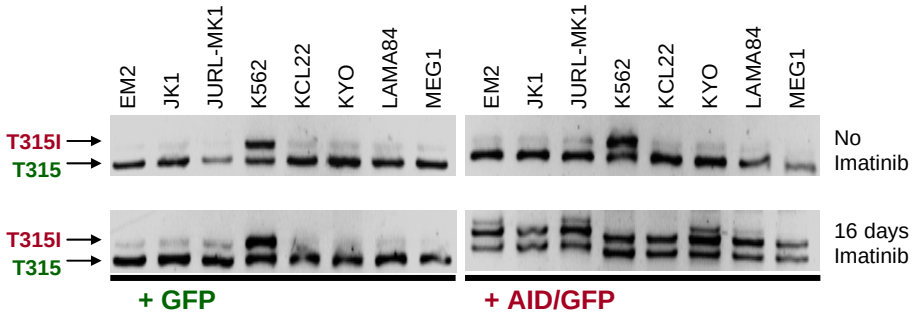

Legend. On the first and last day of treatment with Imatinib, aliquots were taken from *AID*/GFP$^+$ and GFP$^+$ CML cells. *ABL1* exon 6 from *BCR-ABL1* fusions was amplified by PCR and subjected to *Dde*I restriction digest, which distinguishes between wildtype (bottom) and T315I mutant (top) sequences. The PCR product is cleaved in the absence but not in the presence of the T315I mutation. Note that an uncleavable PCR product was obtained from K562 cells even prior to Gleevec-treatment and regardless of AID/GFP- or GFP-transduction, which is consistent with the finding of a pre-existing T315I mutation in these cells (see Table 1).

Figure S5: *Transformation potential of AID$^{-/-}$ and AID wildtype bone marrow B cell precursors by BCR-ABL1*

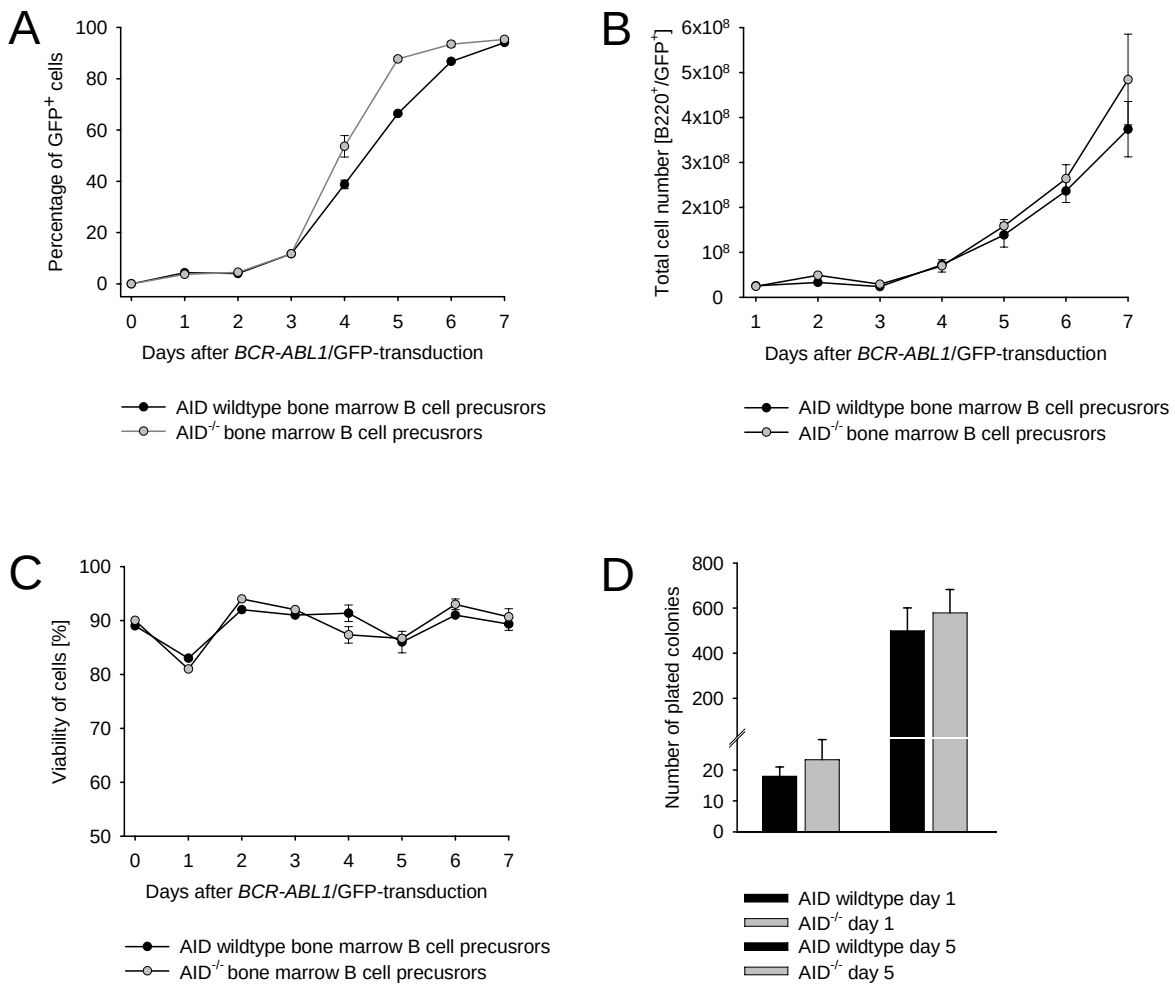

Legend: Bone marrow cells from BALB/CJ wildtype and AID-deficient mice were cultured for 24 h in IMDM with 20% FBS, 50 µM 2-mercaptoethanol and 10 ng/ml IL7. 2.5 x 10^6 cells per well were infected with *BCR-ABL1*-GFP Virus using RetroNectin reagent (Takara Bio, Madison) coated six-well plates. Each well was loaded with *BCR-ABL1*-GFP virus supernatant and the plate was centrifuged at 2000 g for 90 minutes. After the supernatant was removed, we centrifuged the cells at 400 g for 30 minutes on top of the virus loaded plates. Viability (C) and cell count (B; means $\pm$ SD) was determined using a Vi-CELL (Beckman Coulter, Fullerton). The transduction efficiency and the outgrowth of the *BCR-ABL1*-GFP positive cells were measured by FACS (A). The percentage of the total amount of GFP^+ cells and the amount of GFP^+B220^+ cells was determined on a daily base. On day 1 and day 5, a colony-forming cell assay was performed (D; means of colony numbers $\pm$ SD). We prepared a 10X concentrated cell suspension of 2 x 10^5 cells per ml in IMDM. 0.4 ml of cell suspension were added to 4 ml of MethoCult (STEMCELL Technologies, Vancouver). After vortexing, we allowed the bubbles to dissipate before dispensing 1.1 ml of cells + MethoCult mixture using a 3 ml syringe attached to a 16 gauge blunt-end needle to each of three 35 mm dishes. 4 ml of sterile water was added to 2 extra uncovered 35 mm dish. Macroscopic colonies of transformed B cell precursors were counted.

Figure S6: *Sequence analysis of the BCR-ABL1 kinase domain in chronic phase CML and B lymphoid CML blast crisis/Ph$^+$ALL*

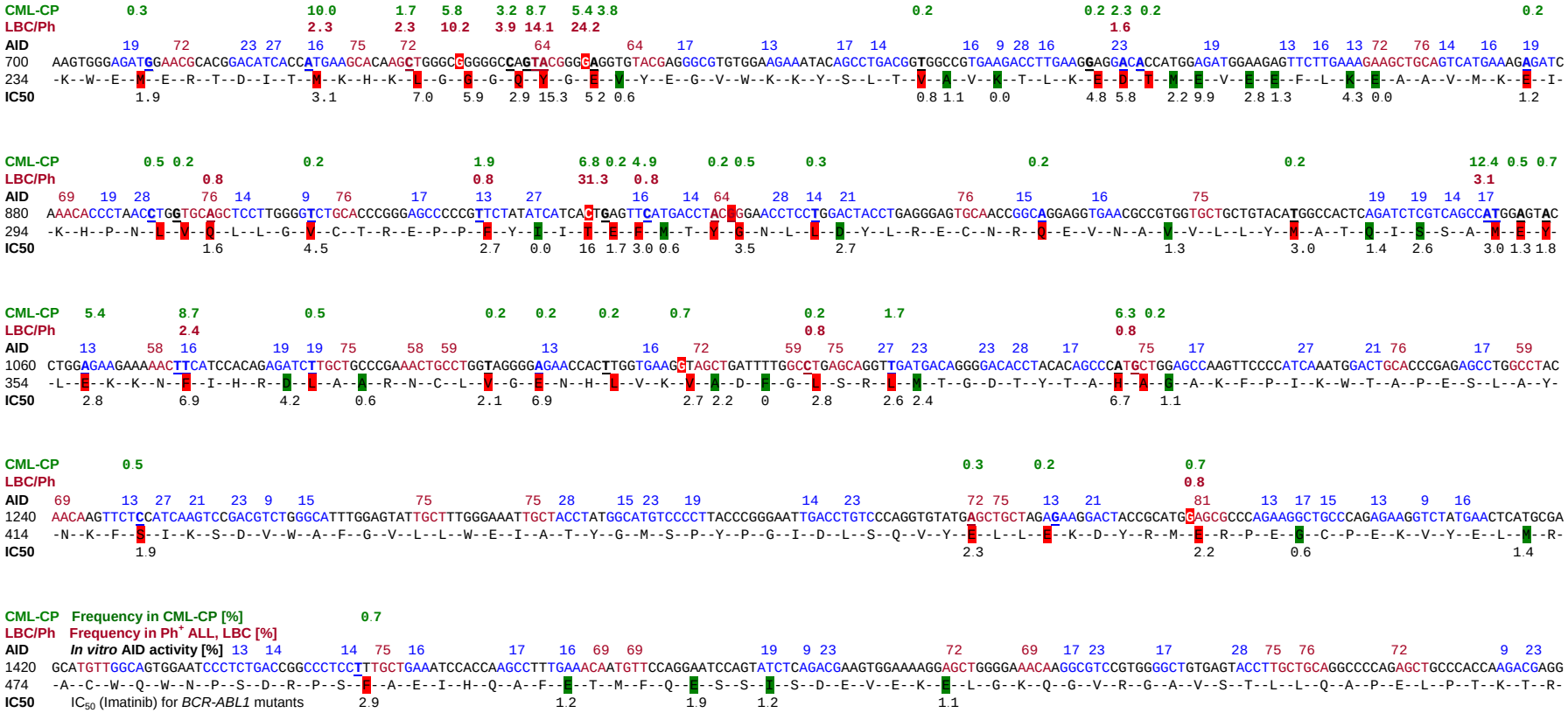

C - C>T and G>A transitions
L - Mutation observed in patients
A - Mutation only observed in *in vitro* mutation screen (Azam et al., 2003)

Control for potential bias resulting from selection effects of individual *BCR-ABL1* kinase mutations: *BCR-ABL1* kinase mutations are subject to strong positive selection, because they provide a selective survival advantage to the leukemia cells in the event of Imatinib-treatment. However, the degree of Imatinib-resistance conferred by individual *BCR-ABL1* kinase mutations is highly variable, which may introduce a bias into our analysis. The possibility of bias was tested based on the following rationale: The degree of Imatinib-resistance conferred by an individual mutation is quantitatively reflected by its IC50 value for Imatinib. Mutations with a particularly strong selective advantage should have a high IC50 value for Imatinib, reflecting a higher degree of drug-resistance. A bias would occur in our analysis, if by chance mutations that represent AID-hotspots also have a high IC50 value. A quantitative measure of AID hotspot targeting was derived from an *in vitro* cytosine deamination assay of AID enzymatic activity using 68 C- or G-based motifs as DNA substrates (Yu et al., 2004; % in vitro deamination indicated in this Figure). For each individual substrate motif, the percentage of AID-induced cytosine deamination provides a quantitative measure of AID hotspot (highlighted in red) or coldspot (highlighted in blue) targeting. To test the possibility of a potential bias in our analysis, we plotted AID-specific mutability (% deamination values indicated here) against IC50 values for all mutations (indicated below amino acide sequence) where both *in vitro* cytosine deamination and IC50 (Imatinib) data were available. The statistical analysis showed that there is no significant correlation between IC50 values and AID targeting (r=0.04; p=0.84; Figure 6F), which argues against the possibility that our analysis is biased by selective advantage of individual mutations.

Figure S7 *B lymphoid-specific gene rearrangements in B lymphoid and myeloid CML blast crisis:*

A.) Analysis of the configuration of the *IGHM* locus including mutation analysis of V region genes

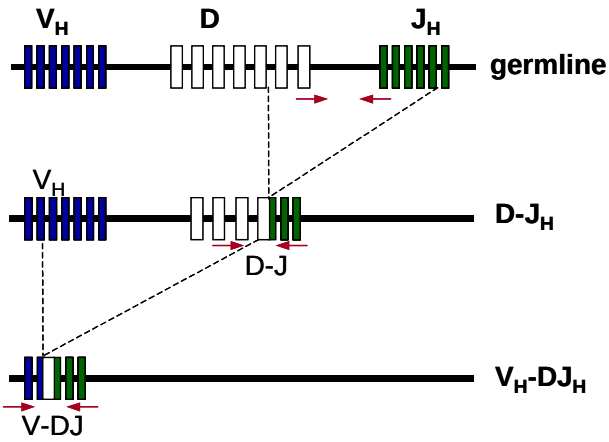

Sample	*IGHM*	Mutations [x10^{-3}bp]	Phenotype
Blank Control	None		None
Normal T cells	Germline		T cell lineage
CML-CP1	Germline		Chronic phase CML
CML-CP2	Germline		Chronic phase CML
CML-CP3	Germline		Chronic phase CML
CML-CP4	Germline		Chronic phase CML
CML-CP5	Germline		Chronic phase CML
CML-CP6	Germline		Chronic phase CML
CML-CP7	Germline		Chronic phase CML
NALM1	V_H1-8-J_H2 V_H3-9-D2-21-J_H5	37 22	B lymphoid blast crisis
BV173	V_H3-21-D2-15-J_H3 Germline	22	B lymphoid blast crisis
LBC1	V_H1-18-D2-2-J_H6 Germline	26	B lymphoid blast crisis
LBC2	V_H1-3-D1-14-J_H4 V_H3-7-D2-2-J_H6	7 15	B lymphoid blast crisis
LBC3	V_H1-8-D5-18-J_H6 Germline	0	B lymphoid blast crisis
LBC4	V_H3-30-D2-15-J_H6	63	B lymphoid blast crisis
LBC5	V_H2-5-J_H5	7	B lymphoid blast crisis
CML-T1	V_H4-34-D2-8-J_H2 Germline	22	T cell/myeloid blast crisis
K562	V_H6-1-D3-9-J_H6	22	Myeloid blast crisis
JURL	Germline		Myeloid blast crisis
EM2	V_H6-1-D3-9-J_H4 V_H1-2-D7-27-J_H4 Germline	3 3	Myeloid blast crisis
LAMA84	V_H6-1-D5-5-J_H3 V_H6-1-D5-18-J_H4 Germline	19 10	Myeloid blast crisis
KYO	Germline		Myeloid blast crisis
KCL22	Germline		Myeloid blast crisis
JK1	V_H6-1-D5-5-J_H4 Germline	21	Myeloid blast crisis
MBC1	V_H3-48-D3-22-J_H4 Germline	48	Myeloid blast crisis
MBC2	V_H3-9-D3-3-J_H3 Germline	37	Myeloid blast crisis
MBC3	Germline		Myeloid blast crisis
MBC4	V_H2-5-D3-16-J_H6 Germline	51	Myeloid blast crisis

B.) Analysis of the configuration of the κ-deleting element (*KDE*) locus including junction analysis

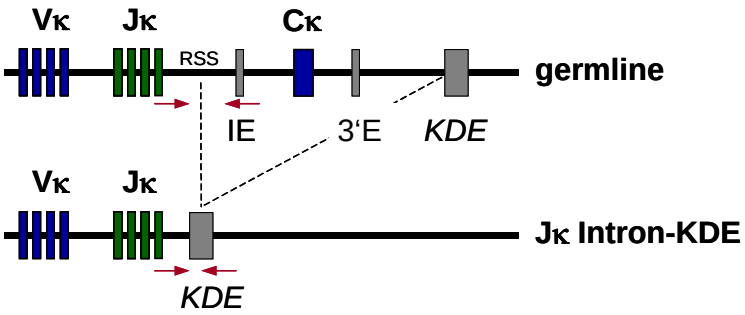

Sample	*KDE*	Phenotype
Blank Control	None	None
T cells	Germline	T cell lineage
CML-CP1	Germline	Chronic phase CML
CML-CP2	Germline	Chronic phase CML
CML-CP3	Germline	Chronic phase CML
CML-CP4	Germline	Chronic phase CML
CML-CP5	Germline	Chronic phase CML
CML-CP6	Germline	Chronic phase CML
CML-CP7	Germline	Chronic phase CML
NALM1	Jκ Intron-KDE	B lymphoid blast crisis
BV173	Jκ Intron-KDE; germline	B lymphoid blast crisis
LBC1	Germline	B lymphoid blast crisis
LBC2	Jκ Intron-KDE; germline	B lymphoid blast crisis
LBC3	Germline	B lymphoid blast crisis
LBC4	Jκ Intron-KDE; germline	B lymphoid blast crisis
LBC5	Jκ Intron-KDE; germline	B lymphoid blast crisis
CML-T1	n.d.	T cell/myeloid blast crisis
K562	Jκ Intron-KDE; germline	Myeloid blast crisis
JURL	Jκ Intron-KDE; germline	Myeloid blast crisis
EM2	Jκ Intron-KDE; germline	Myeloid blast crisis
LAMA84	Jκ Intron-KDE; germline	Myeloid blast crisis
KYO	Germline	Myeloid blast crisis
KCL22	Jκ Intron-KDE; germline	Myeloid blast crisis
JK1	n.d.	Myeloid blast crisis
MBC1	Jκ Intron-KDE; germline	Myeloid blast crisis
MBC2	Jκ Intron-KDE; germline	Myeloid blast crisis
MBC3	Germline	Myeloid blast crisis
MBC4	Jκ Intron-KDE; germline	Myeloid blast crisis

Sequence analysis of *KDE* rearrangements

	Jκ-intron RSS		KDE-RSS
Germline	ATGCTGCCGTAGCCAGCTTTCCTGATG**CACAGTG**		**CACTGTG**GGAGCCCTAGTGGCAGCCCAGGGCGACTCC
NALM1	ATGCTGCCGTAGCCAGC	CCTTCGGG	AGTGGCAGCCCAGGGCGACTCC
BV173	ATGCTGCCGTAGCCAGCTTTCCT	CGTC	GCCCTAGTGGCAGCCCAGGGCGACTCC
LBC2	ATGCTGCCGTAGCCAGCTTTCCTGAT	CC	GAGCCCTAGTGGCAGCCCAGGGCGACTCC
LBC4	ATGCTGCCGTAGCCAGCTTTCC		CCCTAGTGGCAGCCCAGGGCGACTCC
LBC5	ATGCTGCCGTAGCCAGCT	TC	CCTAGTGGCAGCCCAGGGCGACTCC
K562	ATGCTGCCGTAGCCAGCTTTCCTGA		CCCTAGTGGCAGCCCAGGGCGACTCC
JURL	ATGCTGCCGTAGCCAGCTTTCCT	C	GGAGCCCTAGTGGCAGCCCAGGGCGACTCC
EM2	ATGCTGCCGTAGCCAGCTTTCCTGAT	CCGC	TGGGAGCCCTAGTGGCAGCCCAGGGCGACTCC
LAMA84	ATGCTGCCGTAGCCAGCTTTCCTGATG	CT	TGGCAGCCCAGGGCGACTCC
KCL22	ATGCTGCCGTAGCCAGCTTTCCTGA		CTAGTGGCAGCCCAGGGCGACTCC
MBC1	ATGCTGCCGTAGCCAGCTTTCCT	GC	GCCCTAGTGGCAGCCCAGGGCGACTCC
MBC2	ATGCTGCCGTAGCCAGCTTTCCTGATG	CGC	GTGGGAGCCCTAGTGGCAGCCCAGGGCGACTCC
MBC4	ATGCTGCCGTAGCCAGCTTTCC	CT	TGGGAGCCCTAGTGGCAGCCCAGGGCGACTCC

Table S1: *Requirements for AID expression and features of chronic phase and B lymphoid blast crisis CML/Ph$^+$ ALL*

Feature	IgD$^+$	GCB	DLBCL	CML-CP	LBC/Ph$^+$ ALL	Reference
BCR-ABL1	-	-	-	+	+	Heisterkamp *et al*., 1985
NF-κB activation	-	+	+	+	+	Reuther *et al.*, 1998 Gourzi *et al*., 2007 Dedeglu *et al*., 2004
PAX5, E2A	+	+	+	-	+	Gonda *et al.*, 2003 Sayegh *et al.*, 2003 Figure 1C, Figure 5
AID	-	+	+	-	+	Figure 1
ARF deletions	n/a	n/a	+	-	50%	Perrotti,Calabretta, 2004 Figure 3, Figure S2
Aberrant hypermutation *IGHM, BCL6*, *MYC*	-	-	+	-	+	Pasqualucci *et al.,* 2001 Figure 3A
BCR-ABL1 mutations	n/a	n/a	n/a	14%	83%	Soverini *et al.*, 2006 Figure 4, Table 1
DFS (5 years)	n/a	n/a	n/a	87%	4%	Kantarjian et al., 2002; Druker *et al.,* 2006

Notes: IgD$^+$, naïve B cell; GCB, germinal center B cell, DLBCL, Diffuse large B cell lymphoma (GC-derived); CML-CP, chronic phase CML; LBC, lymphoid blast crisis; DFS, disease-free survival

Table S2: *Metaanalysis of BCR-ABL1 kinase mutations in Ph + ALL/CML-LBC and CML-CP*

BCR-ABL1 **kinase mutations**						**Ph+ ALL and CML-LBC**			**CML-CP**			**References for Ph+ ALL and CML-LBC**													**References for CML-CP**																									
bp	**aa**	**DNA**	**IC50**	**AID activity**	**C>T; G>A**	**Cases**	**%**	**C>T; G>A**	**Cases**	**%**	**C>T; G>A**	1	2	3	4	5	6	7	8	9	10	11	12	13	14	1	2	3	15	16	17	18	19	20	21	22	23	24	25	26	27	10	28	29	30	31	32	11	12	33
711	M237I	711G>T	1.9	19		0	0.0		2	0.3																		2																							
730	M244V	730A>G	3.1	16		3	2.3		57	10.0						1						2						1			6	5		1	7	1	6		5	9	1	1	1	1		1	2	9		
742	L248V	742C>G	7	72		3	2.3		10	1.7												1		2				1			2	3					1							2				1		
749	G250E	749G>A	5.9		Y	13	10.2	10.2	33	5.8	5.8	1								5		6		1				2				9			2	10		3	2			1				2	2		
749.5	G250A	749G>C	1.4			0	0.0		7	1.2																1													5							1				
754	Q252E	754C>G	2.9			0	0.0		1	0.2																																				1				
754.5	Q252R	754C>A				3	2.3		4	0.7											1	2																	3								1			
756	Q252H	756G>C				2	1.6		13	2.3						1				1								6			1			1	3		1			1								
757	Y253H	757T>C	15.3	64		17	13.3		39	6.8		1				4				2		7	2	1	1	1			3	5	6		4	4	1	4		4			1		1	1	2			1
758	Y253F	758A>T	3.5	64		1	0.8		11	1.9											1							2			1	2			1									1	2	2		
763	E255K	763G>A	5.2		Y	31	24.2	24.2	31	5.4	5.4	1				1			4	6	4	2	9	3	1	1	2	4			5	6		2	2	1				4		1				1	1	1		
764	E255V	764A>T	18			0	0.0		22	3.8																		1			2	2	1	3	3		2			1						2	2	1	1
767	V256A	767T>G	0.6			0	0.0		0	0.0																																								
802	V268A	802T>G	0.8			0	0.0		1	0.2																												1											
805	A269V	805G>T	1.1			0	0.0		0	0.0																																								
812	K271N	812G>C	0	9		0	0.0		0	0.0																																								
823	E275Q	823G>C	4.8			0	0.0		1	0.2																															1									
827	D276G	827A>G	5.8	23		2	1.6		13	2.3										1		1							3		1					2	2		3							1		1
829	T277A	829A>IG		23		0	0.0		1	0.2																					1																		
832	M278L	832A>T	2.2			0	0.0		0	0.0																																								
838	E279K	838G>A	9.9	19	Y	0	0.0	0.0	0	0.0	0.0																																							
841	E281K	841G>A	2.8		Y	0	0.0	0.0	0	0.0	0.0																																							
844	E282D	844G>T	1.3			0	0.0		0	0.0																																								
855	K285N	855A>C	4.3	13		0	0.0		0	0.0																																								
856	E286K	856G>A	0	72	Y	0	0.0	0.0	0	0.0	0.0																																							
875	E292V	875A>T	1.2	19		0	0.0		1	0.2																												1											
892	L298V	892C>G				0	0.0		3	0.5																												1			1							
895	V299L	895G>T				0	0.0		1	0.2																												1											
899	Q300R	899A>G	1.6	76		1	0.8		0	0.0					1																																		
900	Q300H	900G>C	1.6	76		0	0.0		0	0.0																																								
911	V304G	911T>G	4.5	9		0	0.0		1	0.2																			1																				
931	F311L	931T>C	2.7	13		1	0.8		11	1.9										1											1						2			1	2				2	1	2		
937	I313V	937A>G	0	27		0	0.0		0	0.0																																								
944	T315N	944C>A				0	0.0		2	0.3																1											1												
944.5	T315I	944C>T	16		Y	40	31.3	31.3	39	6.8	6.8	2	1	1		6	6	3	1	4	4	7	2	3				1			4	5		4	3	1	2		2	9	3	2	1					2		
948	E316D	948G>T	1.7			0	0.0		1	0.2																												1												
951	F317L	951C>G	3	16		1	0.8		28	4.9										1							1	2			1	4					7		3	5		3				1	1		
954	M318L	954A>T	0.6	14		0	0.0		0	0.0																																								
959	Y320C	959A>G		64		0	0.0		1	0.2																															1									
962	G321E	962G>A	3.5	64	Y	0	0.0	0.0	3	0.5	0.5																			3																			
971	L324Q	971T>A				0	0.0		2	0.3																					1								1									
973	D325H	973G>C	2.7	21		0	0.0		0	0.0																																								
998	Q333R	998G>A		15		0	0.0		1	0.2																																			1					
1013	V338G	1013T>G	1.3			0	0.0		0	0.0																																								
1028	M343T	1028T>C	3			0	0.0		1	0.2																												1												
1038	Q346H	1038G>C	1.4	19		0	0.0		0	0.0																																								
1043	S348L	1043T>G	2.6	19		0	0.0		0	0.0																																								
1052	M351T	1052T>C	3	17		4	3.1		71	12.4												4				2	3	8	1	1	3	7	6		4		2	3	1	5	9	2	4			2		1	7		
1055	E352G	1055A>G	1.3			0	0.0		3	0.5																				3																				
1057	Y353H	1057T>C	1.8			0	0.0		4	0.7																				2								2											
1064	E355G	1064A>G	2.75	13		0	0.0		31	5.4																		3			2	4		1			7			6			1			1	1	5		
1075	F359I	1075T>A	7.3	16		1	0.8		11	1.9												1				1					1		2			2	2	1		1								1
1075.5	F359V	1075T>G	6.9	16		2	1.6		39	6.8						1						1				1		2			2	1	7			2	1	1			5		2	1			1	1	11		1
1088	D363G	1088A>G	4.2	19		0	0.0		0	0.0																																								
1090	L364I	1090T>A		19		0	0.0		3	0.5																												2			1								
1097	A366D	1097C>A	0.6			0	0.0		0	0.0																																								
1112	V371A	1112T>C	2.1			0	0.0		1	0.2																				1																				
1118	E373G	1118A>G	6.9	13		0	0.0		1	0.2																				1																				
1125	L376V	1125T>G				0	0.0		1	0.2																															1									
1129	V379I	1129G>A	2.7		Y	0	0.0	0.0	4	0.7	0.7																						4									0								
1138	A380S	1138G>T	2.2	72		0	0.0		0	0.0																																								
1146	F382L	1146T>A	0			0	0.0		0	0.0																																								
1150	L384M	1150C>A	2.8	59		1	0.8		1	0.2											1																													1
1159	L387M	1159T>A	2.6	27		0	0.0		10	1.7																						3				1	2			1		1					1		1
1162	M388L	1162A>C	2.4	23		0	0.0		0	0.0																																								
1187	H396P	1187A>C	6.7			1	0.8		1	0.2														1													1												
1187.5	H396R	1187A>G	1.8			0	0.0		35	6.1																1		1			1	5	2		1	10		3			3		1			1	2	4		
1189	A397P	1189G>C		75		0	0.0		1	0.2																																								1
1192	G398R	1192G>A	1.1		Y	0	0.0	0.0	0	0.0	0.0																																							
1250	S417Y	1250C>A	1.9	13		0	0.0		3	0.5																		1			1																	1		
1349	E450G	1349A>G	2.3	72		0	0.0		2	0.3																						2																		
1357	E453Q	1357G>C		13		0	0.0		1	0.2																												1												
1375	E459K	1375G>A	2.2	81	Y	1	0.8	0.8	4	0.7	0.7		1															1										3											
1381	G463D	1381G>A	0.6	17	Y	0	0.0	0.0	0	0.0	0.0																																							
1416	M472I	1416G>C	1.4			0	0.0		0	0.0																																								
1457	F486S	1457T>C	2.9	14		0	0.0		4	0.7																		1										2										1		
1481	E494A	1481G>C	1.2	16		0	0.0		0	0.0																																								
1495	E499K	1495G>A	1.9		Y	0	0.0	0.0	0	0.0	0.0																																							
1506	I502M	1506C>G	1.2	19		0	0.0		0	0.0																																								
1527	E509D	1527G>C	1.1	72		0	0.0		0	0.0																																								
80 unique mutations						**128 cases**		**66.4**	**572 cases**		**19.9**											**128 cases**																											**572 cases**		

Footnotes: bp, base pair; aa, amino acid; DNA, nucleotide position

References for numbers in the Table are given below:

Complete references are listed in Supplemental References.

1 Branford et al., 2002
2 Branford et al., 2003
3 Chien et al., 2008
4 Grammatico et al., 2009
5 Jones et al., 2008
6 Gorre et al., 2001
7 Gorre et al., 2001a
8 Hofmann et al., 2002
9 Pfeifer et al., 2007
10 Shah et al., 2002.
11 Soverini et al., 2006
12 von Bubnoff et al., 2002
13 This study
14 Al-Ali et al., 2004
15 Chu et al., 2005
16 Deininger et al., 2004
17 Ernst et al., 2004
18 Guilhot et al., 2007
19 Hochhaus et al., 2001
20 Hochhaus et al., 2002
21 Hochhaus et al., 2007
22 Irving et al., 2004
23 Jabbour et al., 2006
24 Jiang et al., 2007
25 le Coutre et al., 2008
26 Nicolini et al., 2006
27 Roche-Lestienne et al., 2002
28 Sherbenou et al., 2007
29 Sherbenou et al., 2008
30 Sorel et al., 2004
31 Soverini et al., 2004
32 Soverini et al., 2005
33 Wang et al., 2006

Table S3: *Immunophenotype of patient derived CML samples*

Patient	Age, sex	Blasts [%]	CD10 [%]	CD19	CD24	TdT	CD13 [%]	CD15	CD33	CD54	CD64	CD65	MPO	CD34 [%]
Early B lymphoid blast crisis														
I	62, female	22	44	19	91	22	35	37	32	26	39	43	n.d.	8
II	72, male	28	24	21	n.d.	11	15	10	4	n.d.	n.d.	12	4	18
III	male	25	32	14	29	19	64	29	59	78	n.d.	63	n.d.	19
IV	female	27	31	18	42	12	50	38	44	76	n.d.	48	23	24
Late B lymphoid blast crisis														
V	51, male	70	78	73	59	58	33	2	22	55	2	12	n.d.	76
VI	28, female	84	83	80	91	73	22	20	11	49	11	10	n.d.	43
VII	79, male	87	93	85	94	78	21	10	10	65	10	10	n.d.	70
VIII	24, female	81	84	79	87	74	22	n.d.	24	73	n.d.	11	n.d.	13
Chronic phase CML														
IX	male	4	2	1	15	1	45	34	30	83	55	67	n.d.	9
X	female	8	1	1	23	0	56	41	42	78	60	63	n.d.	12

Notes: TdT, terminal deoxynucleotidyl transferase; MPO, myeloperoxidase; FACS analyses of surface antigens, TdT and MPO are gated on leukemic blasts, percentages refer to positive cells among leukemic blasts. $CD34^+$ $CD13^-$ $CD19^+$ B lymphoid or $CD34^+$ $CD13^+$ $CD19^-$ myeloid leukemic blasts were sorted from bone marrow samples, using a FACStar 440.
The definition of "**Early B lymphoid blast crisis**" is based on the WHO criteria for staging of CML (>20% blasts within the bone marrow; Cortes *et al*., 2006). The traditional classification by Sokal *et al*. (1988) uses 30% bone marrow blasts as cut off. Therefore, the four samples studied here (22% to 28% leukemic blasts) are referred to as "early B lymphoid blast crisis". Samples from these particular patients were chosen for analysis because they included chronic phase CML cells and also a subpopulation of B lymphoid blasts, which indicate the onset of lymphoid blast crisis

Table S4: *Summary of oligonucleotides used for DNA-mutation analysis, RT-PCR and ligation-mediated PCR*

Human *IGHM*

V_H1	5′-CAGTCTGGGGCTGAGGTGAAGA-3'
V_H2	5′-GTCCTRCGCTGGTGAAACCCACACA-3′
V_H3	5′-GGGGTCCCTGAGACTCTCCTGTGCAG-3′
V_H4	5′-GACCCTGTCCCTCACCTGCRCTGTC-3′
V_H5	5′-AAAAAGCCCGGGGAGTCTCTGARGA-3′
V_H6	5′-ACCTGTGCCATCTCCGGGGACAGTG-3′
Cμ	5′-AGACGAGGGGGAAAAGGGTT-3′
J_H1.2.4.5	5′–ACCTGAGGAGACGGTGACCAGGGT–3′
J_H3	5′–ACCTGAAGAGACGGTGACCATTGT–3′
J_H6	5′–ACCTGAGGAGACGGTGACCGTGGT–3′

Human *IGHM* spectratyping primers

V_HFRIIICONS	5′-ACACGGCYSTGTATTACTGT-3′
Cμ	5′-TCAGGACTGATGGGAAGC-3′
Cμ Run off	5′-FAM-GCTGCTGATGTCAGAGTTGT-3′

Human *KDE* rearrangements

KDE germline	5'-CTCACTGAGCCTCCCTTGAATAGTCC-3'
Jκ-Cκ intron	5'-CCGCGGTTCTTTCTCGATTGAGTGG-3'
KDE_R1	5'-CTTCATAGACCCTTCAGGCACATGC-3'
KDE_R2	5'-AGACAGGTCCTCAGAGGTCAGAGC-3'

Human genomic DNA mutation analysis

*MYC*1 F	5'-CACCGGCCCTTTATAATGCG-3'
MYC 1 R	5'-CGATTCCAGGAGAATCGGAC-3'
MYC 2 F	5'-CTTTGTGTGCCCCGCTCCAG-3'
MYC 2 R	5'-GCGCTCAGATCCTGCAGGTA-3'
BCL6 F	5'-ATGCTTTGGCTCCAAGTT-3'
BCL6 R	5'-CACGATACTTCATCTCATC-3'

***BCR-ABL1* Single-cell RT-PCR and mutation analysis**

BCR exon 13	5'-TTCAGAAGCTTCTCCCTGACAT-3'
ABL1 exon 9	5'-CTTCGTCTGAGATACTGGATTCCT-3'
ABL1 exon 4 F	5'-CGAGTTGGTTCATCATCATTC-3'
ABL1 exon 7 R	5'-CTTGATGGAGAACTTGTTGTAGG-3'
ABL1 exon 4 F	5'-GTGGAAGAAATACAGCCTGAC-3'
ABL1 exon 6 R	5′-CTCAGGTAGTCCAGGAGGTTC-3'

***BCR* gene hypermutation analysis**

BCR-F1	5'-AAGGTCAACGACAAAGAGGTGT-3'
BCR-R1	5'-GTCGATCAGGTTGTCCTTCAG-3'
BCR-F2	5'-AAGGTCAACGACAAAGAGGTGT-3'
BCR-R2	5'-AACTCGGCGTCCTCGTAGT-3'

Human RT-PCR primers

GAPDH F	5′-TTAGCACCCCTGGCCAAGG-3′
GAPDH R	5′-CTTACTCCTTGGAGGCCA-3′
BCR-ABL1 F	5′-ACCTCACCTCCAGCGAGGAGGACTT-3'
BCR-ABL1 R	5'-TCCACTGGCCACAAAATCATACAGT-3'

LM-PCR primers

ARF F	5′-CCAGGAATAAAATAAGGGGAATA-3′
ARF F2	5′-GGAATAAAATAAGGGGAATAGGG-3′
ARF R	5′-CTTTCCTACCTGGTCTTCTAGG-3′
V3-21 R	5′-CTCTCGCACAGTAATACACAGC-3′
V1-2 R	5′-CTCTCGCACAGTAATACACGAC-3′
V1-69 R	5′-TCTCTCGCACAGTAATACACG-3′
V3-73 R	5′-GGTTTTCAGGCTGTTCATTT-3′
V3-53 R	5′-CACCTTTTAAAATAGCAACAAGG-3′
V3-30 R	5′-AGCATAGCTACTGAAGGTGAAT-3′
Linker F1	5′-CTGCTCGAATTCAAGCTTCT-3′
Linker F2	5′-GCTTCTAACGATGTACGGGG-3′
Linker R1	5′-GTACATCGTTAGAAGCTTGAA-3′
Linker R2	5′-GTTAGAAGCTTGAATTCGAGC-3′

Human primers for quantitative RT-PCR

SLP65 F	5′-AAAGTCAAAGCACCTCCAAG-3′
SLP65 R	5′-TGTCATCAGCGTTCTCCTC-3′
CD79A F	5′-AAGAACCGAATCATCACAGC-3’
CD79A R	5′-CTGCCCACATCCTGGTAG-3′
PAX5 F	5′-AACTTTTCCCTGTCCATTCC-3′
PAX5 R	5′-GTAGTCCGCCAGAGGATAG-3′
COX6B F	5′-AACTACAAGACCGCCCCTTT-3’
COX6B R	5′-GCAGCCAGTTCAGATCTTCC-3’
AID F	5′–TCCTTTTCACTGGACTTTGG–3′
AID R	5′–GACTGAGGTTGGGGTTCC–3′

Mouse primers for quantitative RT-PCR

Aid F	5'-AAATGTCCGCTGGGCCAA-3'
Aid R	5'-CATCGACTTCGTACAAGGG-3'
Hprt F	5′-GGGGGCTATAAGTTCTTTGC-3′
Hprt R	5′-TCCAACACTTCGAGAGGTCC-3′

Supplemental References

Al-Ali HK, Heinrich MC, Lange T, Krahl R, Mueller M, Müller C, Niederwieser D, Druker BJ, Deininger MW. High incidence of BCR-ABL kinase domain mutations and absence of mutations of the PDGFR and KIT activation loops in CML patients with secondary resistance to imatinib. *Hematol J.* 2004; 5: 55-60.

Azam M, Latek RR, Daley GQ. Mechanisms of autoinhibition and STI-571/imatinib resistance revealed by mutagenesis of BCR-ABL. *Cell*. 2003; 112: 831-43

Blagodatski A, Batrak V, Schmidl S, Schoetz U, Caldwell RB, Arakawa H, Buerstedde JM. A cis-acting diversification activator both necessary and sufficient for AID-mediated hypermutation. *PLoS Genet.* 2009; 5:e1000332.

Branford S, Rudzki Z, Walsh S, Grigg A, Arthur C, Taylor K, Herrmann R, Lynch KP, Hughes TP. High frequency of point mutations clustered within the adenosine triphosphate-binding region of BCR/ABL in patients with chronic myeloid leukemia or Ph-positive acute lymphoblastic leukemia who develop imatinib (STI571) resistance. *Blood.* 2002; 99: 3472-5.

Branford S, Rudzki Z, Walsh S, Parkinson I, Grigg A, Szer J, Taylor K, Herrmann R, Seymour JF, Arthur C, Joske D, Lynch K, Hughes T. Detection of BCR-ABL mutations in patients with CML treated with imatinib is virtually always accompanied by clinical resistance, and mutations in the ATP phosphate-binding loop (P-loop) are associated with a poor prognosis. *Blood.* 2003; 102: 276-83.

Calabretta B, Perrotti D. The biology of CML blast crisis. *Blood.* 2004; 103: 4010-22

Chien JH, Tang JL, Chen RL, Li CC, Lee CP. Detection of BCR-ABL gene mutations in Philadelphia chromosome positive leukemia patients resistant to STI-571 cancer therapy. *Leuk Res.* 2008; 32: 1724-34.

Chu S, Xu H, Shah NP, Snyder DS, Forman SJ, Sawyers CL, Bhatia R. Detection of BCR-ABL kinase mutations in CD34+ cells from chronic myelogenous leukemia patients in complete cytogenetic remission on imatinib mesylate treatment. *Blood.* 2005; 105: 2093-8.

Cortes JE, Talpaz M, O'Brien S, Faderl S, Garcia-Manero G, Ferrajoli A, Verstovsek S, Rios MB, Shan J, Kantarjian HM. Staging of chronic myeloid leukemia in the Imatinib era: an evaluation of the World Health Organization proposal. *Cancer*. 2006; 106: 1306-15.

Dedeoglu F, Horwitz B, Chaudhuri J, Alt FW, Geha RS. Induction of activation-induced cytidine deaminase gene expression by IL-4 and CD40 ligation is dependent on STAT6 and NF-κB. *Int Immunol*. 2004; 16: 395-404.

Deininger MW, McGreevey L, Willis S, Bainbridge TM, Druker BJ, Heinrich MC. Detection of ABL kinase domain mutations with denaturing high-performance liquid chromatography. *Leukemia.* 2004; 18: 864-71.

Druker BJ, Guilhot F, O'Brien SG, Kantarjian H, Deininger MW, Silver RT, Goldman JM, Stone RM, Cervantes F, Hochhaus A, et al. Five-year follow-up of patients receiving Imatinib for chronic myeloid leukemia. *N Engl J Med*. 2006; 355: 2408-17.

Ernst T, Erben P, Müller MC, Paschka P, Schenk T, Hoffmann J, Kreil S, La Rosée P, Hehlmann R, Hochhaus A. Dynamics of BCR-ABL mutated clones prior to hematologic or cytogenetic resistance to imatinib. *Haematologica.* 2008; 93: 186-92.

Faili A, Aoufouchi S, Guéranger Q, Zober C, Léon A, Bertocci B, Weill JC, Reynaud CA. AID-dependent somatic hypermutation occurs as a DNA single-strand event in the BL2 cell line. *Nat Immunol.* 2002; 3: 815-21.

Gonda, H., M. Sugai, Y. Nambu, T. Katakai, Y. Agata, K.J. Mori, Y. Yokota, and A. Shimizu. The balance between Pax5 and Id2 activities is the key to AID gene expression. *J Exp Med.* 2003; 198: 1427-1437.

Gorre ME, Mohammed M, Ellwood K, Hsu N, Paquette R, Rao PN, Sawyers CL. Clinical resistance to STI-571 cancer therapy caused by BCR-ABL gene mutation or amplification. *Science*. 2001; 293: 876-80.

Gourzi P, Leonova T, Papavasiliou FN. Viral induction of AID is independent of the interferon and the Toll-like receptor signaling pathways but requires NF-κB. *J Exp Med*. 2007; 204: 259-65.

Grammatico S, Elia L, Peluso AL, Pedace L, Matarazzo M, Vitale A, Rago A, Pane F, Foà R, Cimino G. Increasing the BCR-ABL expression levels and/or the occurrence of ABL point mutations does not always predict resistance to Imatinib Mesylate in BCR-ABL positive acute lymphoblastic leukemia. *Leuk Res*. 2009; 33: e73-4.

Guilhot F, Apperley J, Kim DW, Bullorsky EO, Baccarani M, Roboz GJ, Amadori S, de Souza CA, Lipton JH, Hochhaus A, Heim D, Larson RA, Branford S, Muller MC, Agarwal P, Gollerkeri A, Talpaz M. Dasatinib induces significant hematologic and cytogenetic responses in patients with imatinib-resistant or -intolerant chronic myeloid leukemia in accelerated phase. *Blood*. 2007; 109: 4143-50.

Heisterkamp N, Stam K, Groffen J, de Klein A, Grosveld G. Structural organization of the bcr gene and its role in the Ph' translocation. *Nature.* 1985; 315: 758-61

Hochhaus A, Kreil S, Corbin A, La Rosée P, Lahaye T, Berger U, Cross NC, Linkesch W, Druker BJ, Hehlmann R, Gambacorti- Passerini C, Corneo G, D'Incalci M. Roots of clinical resistance to STI-571 cancer therapy. *Science.* 2001; 293: 2163.

Hochhaus A, Kantarjian HM, Baccarani M, Lipton JH, Apperley JF, Druker BJ, Facon T, Goldberg SL, Cervantes F, Niederwieser D, Silver RT, Stone RM, Hughes TP, Muller MC, Ezzeddine R, Countouriotis AM, Shah NP. Dasatinib induces notable hematologic and cytogenetic responses in chronic-phase chronic myeloid leukemia after failure of imatinib therapy. *Blood.* 2007; 109: 2303-9.

Hofmann WK, Jones LC, Lemp NA, de Vos S, Gschaidmeier H, Hoelzer D, Ottmann OG, Koeffler HP. Ph(+) acute lymphoblastic leukemia resistant to the tyrosine kinase inhibitor STI571 has a unique BCR-ABL gene mutation. *Blood*. 2002; 99: 1860-2.

Irving JA, O'Brien S, Lennard AL, Minto L, Lin F, Hall AG. Use of denaturing HPLC for detection of mutations in the BCR-ABL kinase domain in patients resistant to Imatinib. *Clin Chem*. 2004; 50: 1233-7.

Jabbour E, Kantarjian H, Jones D, Talpaz M, Bekele N, O'Brien S, Zhou X, Luthra R, Garcia-Manero G, Giles F, Rios MB, Verstovsek S, Cortes J. Frequency and clinical significance of BCR-ABL mutations in patients with chronic myeloid leukemia treated with imatinib mesylate. *Leukemia.* 2006; 20: 1767-73.

Jiang X, Saw KM, Eaves A, Eaves C. Instability of BCR-ABL gene in primary and cultured chronic myeloid leukemia stem cells. *J Natl Cancer Inst.* 2007; 99: 680-93.

Jones D, Thomas D, Yin CC, O'Brien S, Cortes JE, Jabbour E, Breeden M, Giles FJ, Zhao W, Kantarjian HM. Kinase domain point mutations in Philadelphia chromosome-positive acute lymphoblastic leukemia emerge after therapy with BCR-ABL kinase inhibitors. *Cancer.* 2008; 113: 985-94.

Kantarjian HM, Cortes J, O'Brien S, Giles FJ, Albitar M, Rios MB, Shan J, Faderl S, Garcia-Manero G, Thomas DA, Resta D, Talpaz M. Imatinib mesylate (STI571) therapy for Philadelphia chromosome-positive chronic myelogenous leukemia in blast phase. *Blood.* 2002; 99: 3547-53.

le Coutre P, Ottmann OG, Giles F, Kim DW, Cortes J, Gattermann N, Apperley JF, Larson RA, Abruzzese E, O'Brien SG, Kuliczkowski K, Hochhaus A, Mahon FX, Saglio G, Gobbi M, Kwong YL, Baccarani M, Hughes T, Martinelli G, Radich JP, Zheng M, Shou Y, Kantarjian H. Nilotinib (formerly AMN107), a highly selective BCR-ABL tyrosine kinase inhibitor, is active in patients with imatinib-resistant or -intolerant accelerated-phase chronic myelogenous leukemia. *Blood.* 2008; 111: 1834-9.

Nicolini FE, Corm S, Lê QH, Sorel N, Hayette S, Bories D, Leguay T, Roy L, Giraudier S, Tulliez M, Facon T, Mahon FX, Cayuela JM, Rousselot P, Michallet M, Preudhomme C, Guilhot F, Roche-Lestienne C. Mutation status and clinical outcome of 89 imatinib mesylate-resistant chronic myelogenous leukemia patients: a retrospective analysis from the French intergroup of CML (Fi(phi)-LMC GROUP). *Leukemia.* 2006; 20: 1061-6.

Pasqualucci, L., Neumeister, P., Goossens, T., Nanjangud, G., Chaganti, R.S., Kuppers, R., and Dalla-Favera, R. Hypermutation of multiple proto-oncogenes in B-cell diffuse large-cell lymphomas. *Nature* 2001; 412, 341-346.

Pfeifer H, Wassmann B, Pavlova A, Wunderle L, Oldenburg J, Binckebanck A, Lange T, Hochhaus A, Wystub S, Brück P, Hoelzer D, Ottmann OG. Kinase domain mutations of BCR-ABL frequently precede imatinib-based therapy and give rise to relapse in patients with de novo Philadelphia-positive acute lymphoblastic leukemia (Ph+ ALL). *Blood.* 2007; 110: 727-34.

Reuther JY, Reuther GW, Cortez D, Pendergast AM, Baldwin AS Jr. A requirement for NF-kappaB activation in Bcr-Abl-mediated transformation. *Genes Dev.* 1998; 12: 968-81.

Roche-Lestienne C, Soenen-Cornu V, Grardel-Duflos N, Laï JL, Philippe N, Facon T, Fenaux P, Preudhomme C. Several types of mutations of the Abl gene can be found in chronic myeloid leukemia patients resistant to STI571, and they can pre-exist to the onset of treatment. *Blood.* 2002; 100: 1014-8.

Sayegh CE, Quong MW, Agata Y, Murre C. E-proteins directly regulate expression of activation-induced deaminase in mature B cells. *Nat Immunol.* 2003; 4: 586-93.

Schlissel M, Constantinescu A, Morrow T, Baxter M, Peng A. Double-strand signal sequence breaks in V(D)J recombination are blunt, 5'-phosphorylated, RAG-dependent, and cell cycle regulated. *Genes Dev.* 1993; 7: 2520-32.

Shah NP, Nicoll JM, Nagar B, Gorre ME, Paquette RL, Kuriyan J, Sawyers CL. Multiple BCR-ABL kinase domain mutations confer polyclonal resistance to the tyrosine kinase inhibitor Imatinib (STI571) in chronic phase and blast crisis chronic myeloid leukemia. *Cancer Cell*. 2002; 2: 117-25

Sherbenou DW, Wong MJ, Humayun A, McGreevey LS, Harrell P, Yang R, Mauro M, Heinrich MC, Press RD, Druker BJ, Deininger MW. Mutations of the BCR-ABL-kinase domain occur in a minority of patients with stable complete cytogenetic response to imatinib. *Leukemia.* 2007; 21: 489-93.

Sherbenou DW, Hantschel O, Turaga L, Kaupe I, Willis S, Bumm T, Press RD, Superti-Furga G, Druker BJ, Deininger MW. Characterization of BCR-ABL deletion mutants from patients with chronic myeloid leukemia. *Leukemia.* 2008; 22: 1184-90.

Sokal J, Baccarani M, Russo D, Tura S (1988). Staging and prognosis in chronic myelogenous leukemia. *Semin Hematol* 25: 49–61.

Sorel N, Bonnet ML, Guillier M, Guilhot F, Brizard A, Turhan AG. Evidence of ABL-kinase domain mutations in highly purified primitive stem cell populations of patients with chronic myelogenous leukemia. *Biochem Biophys Res Commun.* 2004; 323: 728-30.

Soverini S, Martinelli G, Amabile M, Poerio A, Bianchini M, Rosti G, Pane F, Saglio G, Baccarani M; Italian Cooerative Study Group on Chronic Myeloid Leukemia; European LeukemiaNet-6th Framework Program of the European Community. Denaturing-HPLC-based assay for detection of ABL mutations in chronic myeloid leukemia patients resistant to Imatinib. *Clin Chem.* 2004; 50: 1205-13.

Soverini S, Martinelli G, Rosti G, Bassi S, Amabile M, Poerio A, Giannini B, Trabacchi E, Castagnetti F, Testoni N, Luatti S, de Vivo A, Cilloni D, Izzo B, Fava M, Abruzzese E, Alberti D, Pane F, Saglio G, Baccarani M. ABL mutations in late chronic phase chronic myeloid leukemia patients with up-front cytogenetic resistance to imatinib are associated with a greater likelihood of progression to blast crisis and shorter survival: a study by the GIMEMA Working Party on Chronic Myeloid Leukemia. *J Clin Oncol.* 2005; 23: 4100-9.

Soverini S, Colarossi S, Gnani A, Rosti G, Castagnetti F, Poerio A, Iacobucci I, Amabile M, Abruzzese E, et al. Contribution of ABL kinase domain mutations to Imatinib resistance in different subsets of Philadelphia-positive patients: by the GIMEMA Working Party on Chronic Myeloid Leukemia. *Clin Cancer Res*. 2006;12: 7374-9. B

von Bubnoff N, Schneller F, Peschel C, Duyster J. BCR-ABL gene mutations in relation to clinical resistance of Philadelphia-chromosome-positive leukaemia to STI571: a prospective study. *Lancet.* 2002; 359: 487-91.

Wang L, Knight K, Lucas C, Clark RE. The role of serial BCR-ABL transcript monitoring in predicting the emergence of BCR-ABL kinase mutations in imatinib-treated patients with chronic myeloid leukemia. *Haematologica.* 2006; 91: 235-9.

Yu K, Huang FT, Lieber MR. DNA substrate length and surrounding sequence affect the activation-induced deaminase activity at cytidine. *J Biol Chem.* 2004; 279: 6496-500.